Determination of Propagation Rate Coefficients by Pulsed-Laser Polymerization for Systems with Rapid Chain Growth: Vinyl Acetate†

R. A. Hutchinson,* J. R. Richards, and M. T. Aronson

Central Research and Development, E. I. du Pont de Nemours and Co., Inc., Experimental Station, Wilmington, Delaware 19880-0101

Received March 16, 1994; Revised Manuscript Received May 11, 1994®

ABSTRACT: The pulsed-laser polymerization (PLP) technique for determination of free radical propagation rate coefficients (k_p) by gel permeation chromatography analysis has been extended to systems with rapid chain growth. A mathematical model is developed to gain a better understanding of the relative importance of propagation, termination, and transfer events on the laser-generated molecular weight distributions. Insights from the model are used to define appropriate PLP experimental conditions for vinyl acetate (VAc), for which measured k_p values are an order of magnitude higher than values measured for styrene and methyl methacrylate at the same temperature. The behavior of VAc is contrasted with methyl methacrylate, both by experimental means and through simulation. Results suggest that VAc radicals not only propagate quickly but also have a higher rate of termination than methacrylate or styrene monomer systems, explaining the formation of broad, featureless molecular weight distributions under typical PLP experimental conditions. This work demonstrates the value of mathematical modeling to aid in the design of optimal PLP experiments.

Introduction

The pulsed-laser polymerization (PLP) technique is a direct and reliable method for estimating free radical propagation rate coefficients (k_p) from molecular weight distributions (MWDs). The technique, pioneered by Olaj and co-workers,[1,2] involves the exposure of a monomer system with a photoinitiator to laser flashes which generate a periodic profile of polymer radicals. Between flashes, the radical concentration decreases due to radical-radical termination. At the end of the period between flashes (t_0), the radicals which have escaped termination have propagated to a chain length P_0, given by the equation[1]

$$P_0 = k_p[M]t_0 \quad (1)$$

where [M] is the monomer concentration. When the next flash arrives, these radicals are exposed to a high concentration of newly generated radicals, which leads to a greatly increased probability for their termination. Thus, the formation of dead polymer molecules with lengths close to P_0 is favored. With a measure of P_0 using gel permeation chromatography (GPC), k_p can be calculated from eq 1. Proper analysis of the GPC-measured MWD not only yields a direct estimate of k_p but also provides consistency checks as to the validity of the estimate.[3]

This work is the second part of a study to improve and extend the PLP method.[3] The technique has been extensively used to estimate k_p for methacrylate systems[2-6] and styrene.[2-4,7,8] Reported values show not only excellent agreement among themselves, but also consistency with values measured by other, more laborious, techniques. Furthermore, it has been experimentally verified that k_p estimates are independent of laser pulse frequency and monomer concentration.[2,9,10]

The monomers examined in previous work have relatively slow chain growth. Reported k_p values are generally in the range 100–500 L/(mol s); the highest value found in the literature is our previously reported value of 1500 L/(mol s) for methyl methacrylate (MMA) at 90 °C.[3] To date, the technique has not been successfully applied to high k_p systems, such as acrylates or vinyl acetate. Davis *et al.*[11] were unsuccessful in estimating k_p values for the homopolymerization of methyl acrylate and butyl acrylate. The authors state that the PLP-generated MWDs were broad, as opposed to the characteristically sharp peaks obtained with other monomers. We have reported similar results for vinyl acetate (VAc).[3] The nature of the problem is illustrated by Figure 1, which shows MWDs for PMMA and PVAc samples produced by PLP at identical conditions. Whereas the PMMA distribution has a sharp, clearly defined laser-generated peak amenable to analysis (see below), the PVAc distribution is broad and featureless. Unfortunately, no meaningful k_p estimate can be obtained

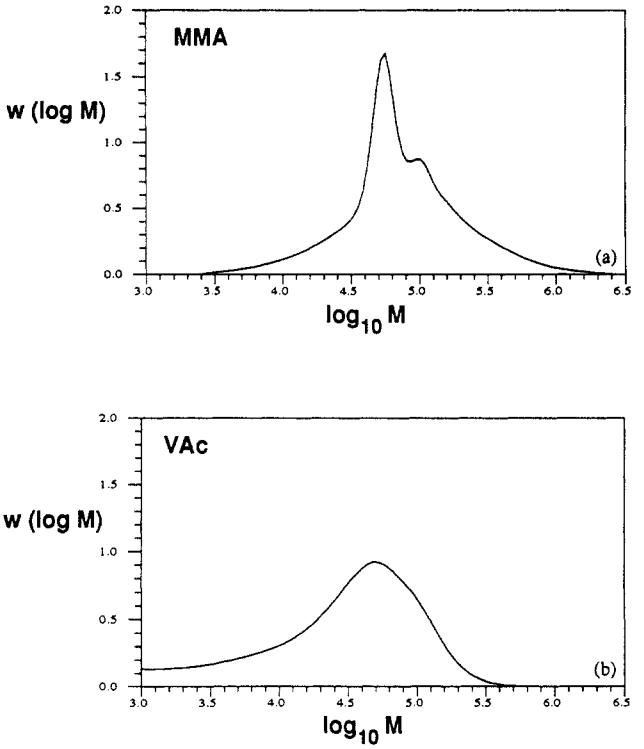

Figure 1. (a) PMMA and (b) PVAc molecular weight distributions produced by pulsed-laser polymerization at identical conditions: t_0 = 0.1 s, T = 40 °C, [benzoin] = 5 mmol/L.

* To whom correspondence should be addressed.
† Part of this work was presented at the 1993 AIChE Annual Meeting, St. Louis, MO.
® Abstract published in *Advance ACS Abstracts*, June 15, 1994.

0024-9297/94/2227-4530$04.50/0

from this distribution.

This paper examines the cause behind the broad MWDs of Figure 1. A mathematical model representing polymerization under pulsed-laser conditions has been developed. The model is compared to previous work in the literature,[1,8,12,13] and simulations comparing the MMA and VAc systems are presented. Insights gained from modeling the PLP systems are used to define appropriate experimental conditions for VAc. With careful analysis of the laser-generated MWDs, a k_p determination has been completed for VAc in the temperature range of 10–40 °C.

Experimental Section

The experimental setup is described in our previous work.[3] A Quanta-Ray pulsed DCR11 Nd:YAG laser with a harmonic generator is used to generate light of wavelength 355 nm at a pulse energy of 70 mJ/pulse and a half-height pulse width of 6 ns. All experiments are run with a pulse repetition rate of 10 Hz (t_o = 0.1 s) for a total time sufficient to allow 0.5–2.0% conversion of monomer to polymer. Monomers (MMA and VAc) and benzoin photoinitiator were used as received.

All GPC analyses were performed at 30 °C using tetrahydrofuran as eluant on a system consisting of a Waters pump (Model 590), a Waters autosampler (WISP 712), two SHODEX columns (KF80M), and a Waters differential refractometer (Model 410). PMMA samples were analyzed on the basis of a calibration curve obtained from narrow-distribution PMMA standards. PVAc analysis was based upon universal calibration using narrow-distribution polystyrene standards and known Mark–Houwink coefficients.[14]

Inflection points are obtained by fitting the experimental MWD with cubic smoothing splines, followed by differentiation of the splines; both tasks are performed using IMSL math library routines.[15] Inflection points are reported for the log scale GPC distribution, as well as the weight distribution transformed to a linear scale. Further details of the analysis procedure have been described previously,[3] and will not be repeated here.

In accordance with theory,[1] the inflection points from the derivative plot (linear scale) are used to calculated k_p, using a rearranged form of eq 1:

$$k_p = \frac{M_o}{1000\rho t_o} \tag{2}$$

where M_o is the polymer MW at the inflection point, k_p has units of L/(mol s) and monomer density ρ has units of g/cm^3. Monomer densities are calculated as a function of temperature (T_c in °C) for MMA[16] and VAc[17] according to

$$\rho_{MMA} = 0.9569 - 1.2129 \times 10^{-3}T_c + 1.6813 \times 10^{-6}T_c^2 - 1.0164 \times 10^{-8}T_c^3 \tag{3}$$

$$\rho_{VAc} = 0.9584 - 1.3276 \times 10^{-3}T_c \tag{4}$$

Model Development

The kinetic scheme used for model development is shown as Figure 2. The scheme includes initiation, propagation, chain transfer to monomer (M) and solvent (S), and termination by combination and disproportionation. P_n and D_n indicate living and dead species of length n, respectively. In order to model the pulsed-laser-generated MWD, it is necessary to formulate and solve differential equations to follow the concentrations of chains of all lengths, with n varying between length 1 and z. The method of moments is used to follow the total chain concentrations in the system; this allows the exact calculation of the full MWD, truncated at chain length z. Details of the model development are presented in the Appendix. The set of differential equations are coded and solved in SPEEDUP, a commercial package for dynamic simulations.

Initiation:

$$I \xrightarrow{h\nu} 2I\cdot$$

$$I\cdot + M \xrightarrow{k_i} P_1$$

Propagation:

$$P_n + M \xrightarrow{k_p} P_{n+1}$$

Chain Transfer:

To Monomer: $$P_n + M \xrightarrow{k_{tr,m}} D_n + P_1$$

To Solvent: $$P_n + S \xrightarrow{k_{tr,s}} D_n + P_1$$

Termination:

$$P_n + P_m \xrightarrow{k_{td}} D_n + D_m$$

$$P_n + P_m \xrightarrow{k_{tc}} D_{n+m}$$

$$P_n + I\cdot \xrightarrow{k_t} D_n$$

$$I\cdot + I\cdot \xrightarrow{k_t} dead$$

$$k_t = k_{tc} + k_{td}$$

Figure 2. Kinetic scheme used for the development of the PLP model.

In addition to the kinetic coefficients listed in Figure 2, it is necessary to input the concentration of radicals generated per pulse, [ΔR•], where [R•] includes radicals present as initiator fragments or growing polymer chains. It is assumed that the new radicals are generated instantaneously at every pulse. Experimentally, radical generation is a function of many factors—laser power, photoinitiator concentration and extinction coefficient, path length, radical efficiencies, impurities, etc. In the model, [ΔR•] is treated as an adjustable parameter. As discussed in previous modeling efforts,[1,13] it is the product of [ΔR•] and k_t which strongly affects the appearance of the MWD.

PLP has been previously modeled by several workers. Olaj and co-workers[1] considered the system in the absence of chain transfer. Theoretical MWDs were calculated analytically by making a transformation between time and chain length. It was shown that the best measure of M_o is given by the inflection point of the distribution and that the position of the inflection point is not sensitive to the mode of termination (combination vs disproportionation). However, their treatment is useful only for systems with negligible chain transfer and does not capture the Poisson broadening of the MWD, which had to be added in an *ad hoc* fashion. Integration of the differential equations in the present work naturally gives rise to Poisson broadening, as was shown by Ray[18] for a living (no termination) polymer system (see Appendix). The numerical solution of the present model was verified using both Ray's analytical solutions for a living polymer system[18] and Olaj's results for PLP in the absence of chain transfer.[1]

Recently, Olaj's pioneering work has been extended by a number of researchers. Lu *et al.*[12] and O'Driscoll and Kuindersma[13] use Monte Carlo techniques to model PLP. The latter work[13] brings out some very important features of the technique, further verifying the conclusion that the inflection point of the PLP-generated peak is a good estimate for M_o, and discussing how the overall appearance of the MWD is governed by the relative rates of photo-

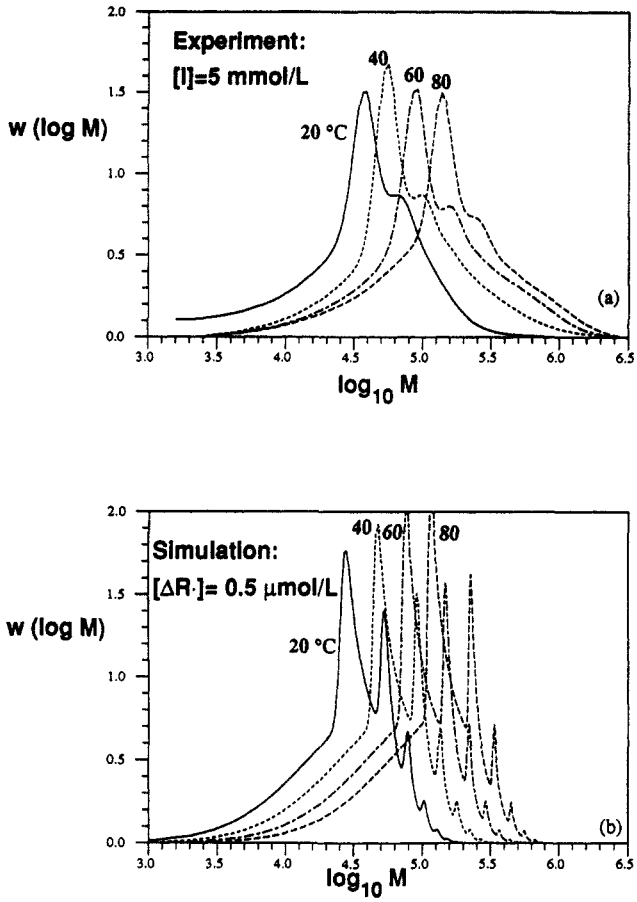

Figure 3. Molecular weight distributions for PMMA produced by pulsed-laser polymerization at 10 Hz and various temperatures: (a) experimental results, [I] = 5 mmol/L; (b) simulation results, with [ΔR·] = 0.5 μmol/L, kinetic parameters from Table 1.

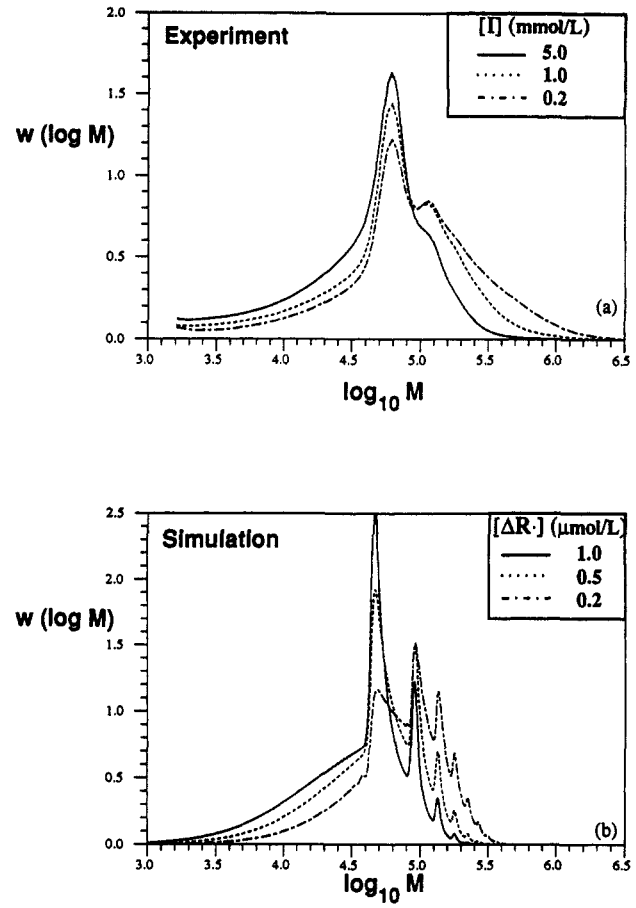

Figure 4. Molecular weight distributions for PMMA produced by pulsed-laser polymerization at 10 Hz and 40 °C: (a) experimental results, varying [I]; (b) simulation results, varying [ΔR·], kinetic parameters from Table 1.

initiation, propagation, and termination. Once again, however, chain transfer effects were not considered.

The present model is most similar in form to one developed in parallel by Deady *et al.*,[8] although few details of their model structure are presented. Like the present work, their kinetic scheme includes chain transfer to monomer, and the set of system differential equations are solved numerically. However, it appears as if the present model uses a much more efficient solution technique and extends to much higher degrees of polymerization. Deady and co-workers[8] typically solve to chain lengths of 160, taking up to 1000 CPU seconds on a Cray YMP-2 supercomputer. The present model takes 1500 CPU seconds on a VAXstation 4000-90 minicomputer to simulate a period of 10 pulses (1 s) for a MMA system, following polymer chains to length 7500. The efficiency of the model makes it a useful tool for guiding experimental work and examining real systems such as MMA or VAc, for which P_0 values are as high as 5000.

Results

MMA. The ability of the model to predict experimental MWDs is illustrated by Figure 3, which shows experimental results presented in our previous work.[3] The simulations of Figure 3 were performed with [ΔR•] at 0.5 μmol/L; other kinetic parameters used in the model are summarized in Table 1. The experimental features of the distributions— sharp primary peaks, smaller secondary peaks, and the effect of temperature—are also seen in the model results. Note that the simulated distribution are much sharper than the experimental curves, with tertiary and higher order peaks clearly visible.

Table 1. Model Parameters for PLP Simulations (Activation Energies in cal/mol)

(L/mol-s)	MMA	VAc[16]
k_p	$2.39 \times 10^6 \exp(-5300/RT)$[3] [480 @ 40 °C]	1500–6000 @ 40 °C
k_t	$1.47 \times 10^8 \exp(-701/RT)$[19] [$5 \times 10^7$ @ 40 °C]	10^7–10^9
k_{t_c}	0.0	0.0
$k_{tr,m}/k_p$	$7.4 \times 10^{-2} \exp(-5670/RT)$[19] [$8 \times 10^{-6}$ @ 40 °C]	2×10^{-4} @ 40 °C
k_i	$10k_p$	$10k_p$

Simulations by O'Driscoll and Kuindersma[13] illustrate how the shape of PLP-generated distributions are affected by the relative magnitude of chain growth and termination. Although the values of k_p and k_t (termination rate coefficient) for a given monomer are fixed, it is possible to alter the value of [ΔR•] in the system. One method to do this experimentally is to vary the photoinitiator concentration, [I]. Figure 4 shows the effects of [I] on PMMA MWDs produced by PLP at 40 °C. Decreasing [I] results in a deceased intensity for the primary peak, and an increased intensity for the secondary peak. As expected, the position of the peaks (and their inflection points) remains unchanged. Once again, the simulation results follow the experimentally observed trends. Figure 4 illustrates that it is possible to exert a measure of experimental control over the shape of the PLP-generated MWD.

VAc vs MMA. With confidence in the model's ability to predict experimental trends, a comparison of the VAc and MMA systems is possible. Although there is a wide range of reported kinetic values for VAc (summarized in

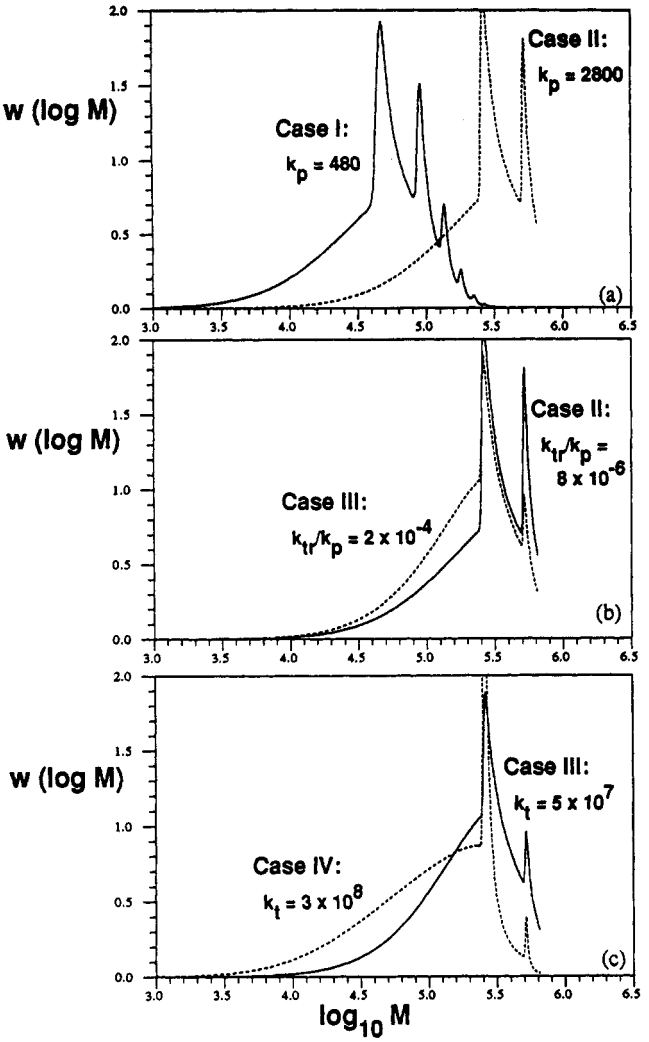

Figure 5. Effect of kinetic parameters on simulated PLP-generated MWDs (T = 40 °C, [ΔR·] = 0.5 μmol/L): (case I) MMA parameters; (case II) same as I, with VAc density and MW, k_p = 2800; (case III) same as II, with $k_{tr,m}/k_p = 2 \times 10^{-4}$; (case IV) same as III, with $k_t = 3 \times 10^8$.

Table 1), it is clear that it has much higher k_p and k_{tr_m} (chain transfer to monomer rate coefficient) values than MMA. The individual kinetic parameters have been systematically varied in order to examine their relative importance on the PLP-generated MWDs through simulation; results are shown in Figure 5.

Figure 5a compares the simulated MMA distribution at 40 °C (case I) to a distribution with k_p increased by a factor of 5.8, k_{tr_m}/k_p and k_t unchanged (case II). While the higher k_p value shifts the distribution to higher MWs (see eq 1), its shape remains unchanged. It can be concluded that high k_p values alone cannot cause the difficulties observed with the VAc system illustrated by Figure 1.

Davis *et al.*[11] hypothesize that a high rate of chain transfer to monomer causes the formation of broad, featureless PLP-generated MWDs. To examine this hypothesis, case II is replotted in Figure 5b, along with case III, for which k_{tr_m}/k_p is increased to a value typical for VAc (25 times higher than the MMA value). Simulations show that the increased chain transfer to the monomer creates a significant buildup of lower MW material, as evidenced by the appearance of a shoulder on the distribution. Although the secondary peak greatly decreases in intensity, the height and breadth of the primary peak remains largely unchanged. On the basis of these simulations, it can be concluded that chain transfer

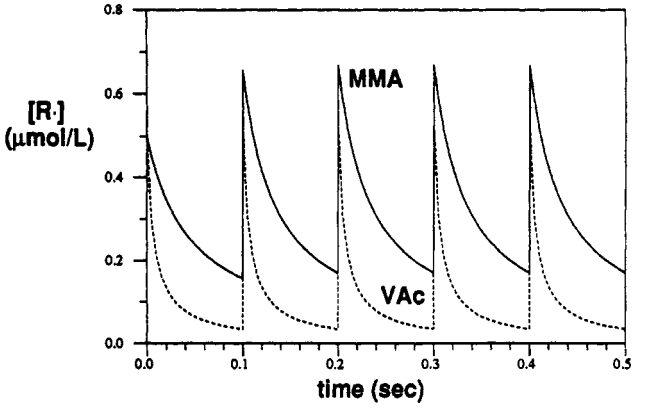

Figure 6. Radical profiles for simulations of Figure 5: MMA (case I) and VAc (case IV).

to VAc monomer is not sufficient to explain the observed experimental difficulties.

Estimates for VAc k_t values[16] vary in the range 10^7–10^9. In Figure 5c, the effect of increasing k_t by a factor of 6 (case IV) is compared to case III. The simulations indicate that increased termination has a dramatic effect on the PLP-generated MWD, causing the formation of additional low MW material and broadening the distribution. It also has a significant effect on the primary PLP peak, which narrows to almost a spike. In general, this spike may not be visible experimentally due to peak broadening in the GPC column.[20]

Figure 5 shows that although transfer to monomer broadens the distribution, it is the termination events which control the appearance of the PLP-generated MWD for VAc. The importance of k_t is further illustrated in Figure 6, a plot of radical concentration for the MMA (case I) and VAc (case IV) simulations of Figure 5. For MMA, about 25% of the growing radicals are still alive when the next pulse arrives; for VAc the value is less than 7%. It is believed that the remaining fraction of radicals is simply too low to create an observable PLP k_p peak. Experimental evidence presented below strongly supports this hypothesis. Without the model, this effect would be difficult to explain.

VAc. Simulation results suggest that the rate of termination is very high for the VAc system so that, under typical PLP experimental conditions, an insufficient fraction of radicals survive until the next pulse. As shown in the Appendix, this surviving fraction (here denoted by β), is given by

$$\beta = \frac{1}{1 + k_t[\mathrm{R}^\bullet]_{max} t_o} \tag{5}$$

where $[\mathrm{R}^\bullet]_{max}$ is the radical concentration immediately following a laser pulse. From this equation, it can be seen that one possible solution to this problem is to decrease t_o, the time between pulses; the effect of t_o on the shape of MWDs has been demonstrated by Zifferer and Olaj for systems initiated by the rotating sector technique.[23] However, since our particular laser is limited to a maximum pulse rate of 10 Hz, we turned to a second means of increasing β—a decrease in $[\mathrm{R}^\bullet]_{max}$, accomplished experimentally by decreasing [I]. Figure 7 shows how the MWDs for VAc pulsed at 20 °C shift to the right as [I] is decreased. Indeed, after [I] is decreased by a factor of 25 to 0.2 mmol/L, a multimodal distribution becomes apparent, which is then invariant with a further decrease of [I] to 0.04 mmol/L. It is only at these much reduced photoinitiator concentrations that the true k_p peak for VAc becomes

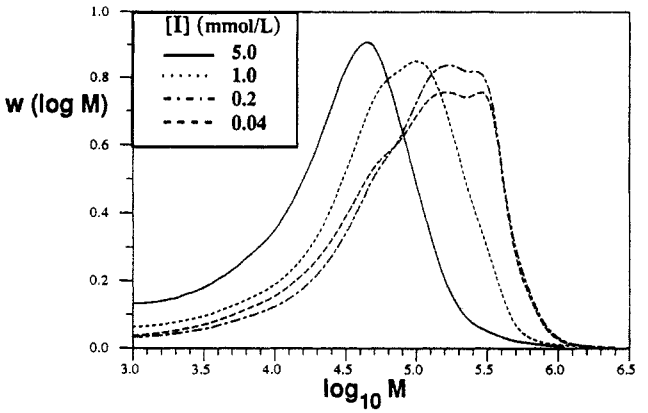

Figure 7. Effect of initiator concentration on PLP-generated MWDs for VAc: T = 20 °C, t_0 = 0.1 s.

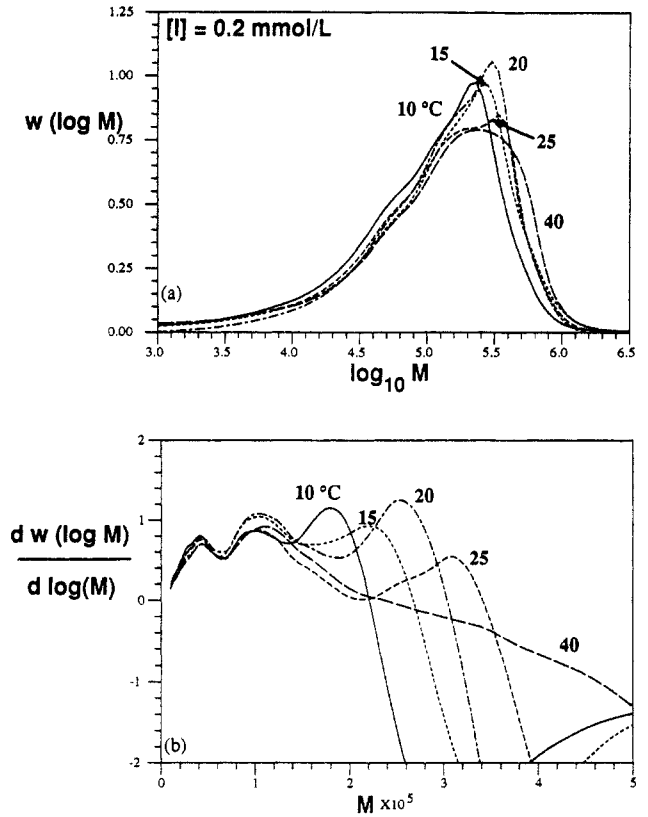

Figure 8. PVAc produced by pulsed-laser polymerization with [I] = 0.2 mmol/L: (a) mass MWDs; (b) derivative plots.

detectable. The sensitivity to initiator concentration can be contrasted with that of the MMA system (Figure 4).

A series of experiments were carried out at various temperatures with [I] = 0.2 mmol/L. Typical distributions and derivative plots are shown as Figure 8; inflection points and estimated k_p values are summarized in Table 2. Although the distributions appear to be almost superimposed on each other, a clear shift of the primary inflection point with temperature is evident in the derivative plots. The tabulated k_p inflection points are well fit by an Arrhenius relationship:

$$\ln(k_p) = (19.4 \pm 0.7) - (3350 \pm 200)/T \quad (6)$$

or

$$k_p\ (\mathrm{L \cdot mol^{-1} \cdot s^{-1}}) = 2.7 \times 10^8 \exp\left(\frac{-6650\ \mathrm{cal \cdot mol^{-1}}}{RT}\right) \quad (7)$$

The cause of the lower MW inflection points at 4×10^4 and 1×10^5 is unknown. However, these inflection points

Table 2. Inflection Points from PLP-Generated MWDs for Bulk VAc (t_0 = 0.1 s)[a]

T (°C)	M_0 (log MWD)	M_0 (linear MWD)	k_p (L/(mol s))
10	179 000	183 000	1940
	176 000	182 000	1930
15	219 000	229 000	2440
	215 000	219 000	2340
20	253 000	258 000	2770
	253 000	261 000	2800
	269 000	290 000	3110
	274 000	286 000	3070
	244 000	280 000	3000
	250 000	282 000	3030
	260 000	280 000	3000
	272 000	285 000	3060
25	309 000	318 000	3460
	304 000	313 000	3380

[a] k_p values are calculated using the inflection point from the linear MWD.

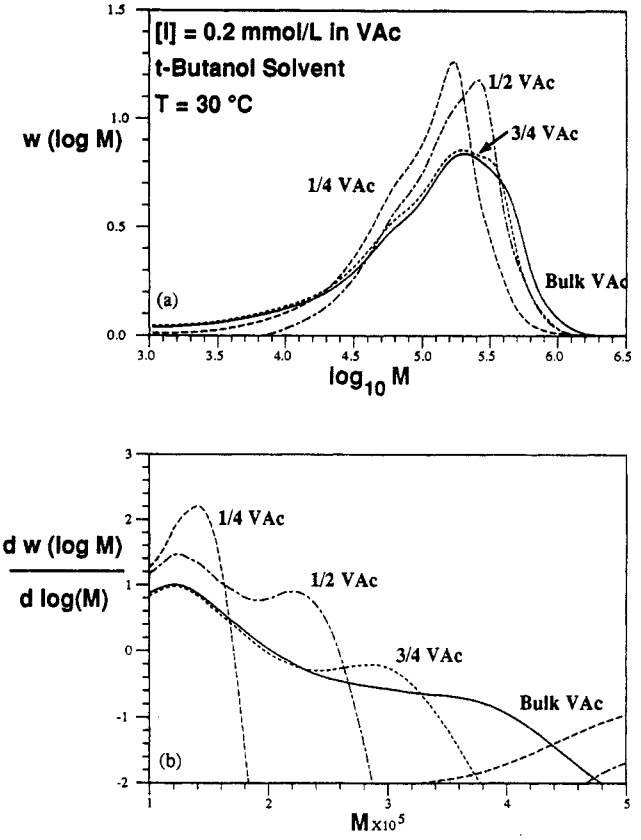

Figure 9. PVAc produced by pulsed-laser polymerization at 30 °C in *tert*-butyl alcohol diluent: (a) mass MWDs; (b) derivative plots. [I] = 0.2 mmol/L in VAc. Labels refer to the VAc volume fraction in the sample.

are temperature invariant and do not correspond to the main peak of the MWD, strongly suggesting that they are not related to the determination of k_p. These points also offer no particular difficulties in the data analysis, since they are far removed from the primary maximum in the MWD.

Even with a low photoinitiator concentration, it is difficult to obtain inflection points above a temperature of 25 °C, as shown by the 40 °C curve in Figure 8. To bring the inflection points down to a lower MW region, higher temperature experiments were performed in *tert*-butyl alcohol diluent. As can be seen from eq 1, reducing [M] results in a decrease in the characteristic chain length, P_0. *tert*-Butyl alcohol was chosen as the diluent because it exhibits relatively low chain transfer rates with VAc.[16] Typical results are shown in Figure 9, for T = 30 °C. As

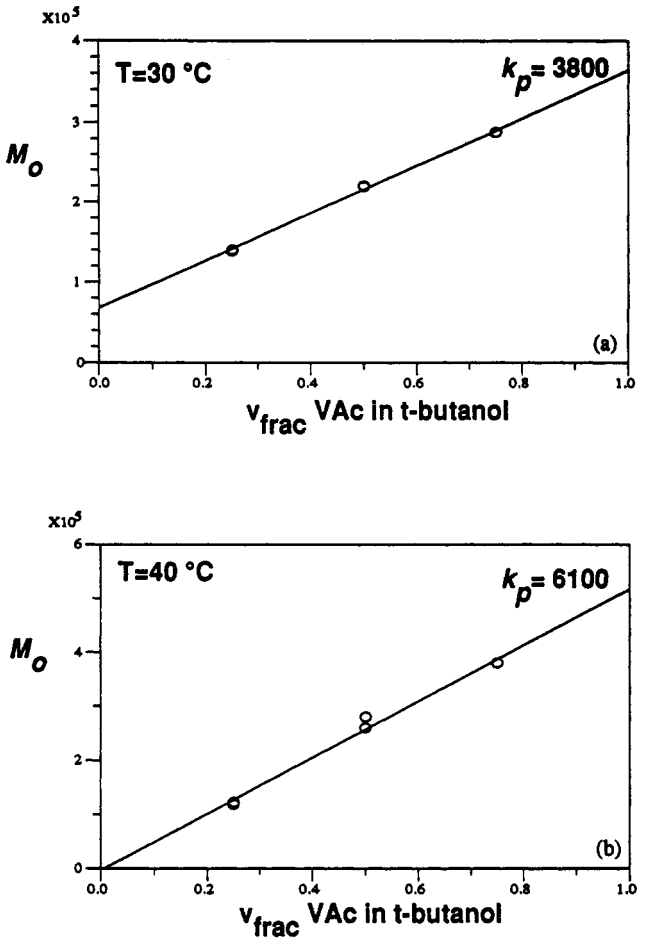

Figure 10. Critical inflection point (M_o) as a function of VAc volume fraction in VAc/*tert*-butyl alcohol solution: (a) 30 °C; (b) 40 °C. k_p values calculated from regression fits (lines) extrapolated to pure VAc.

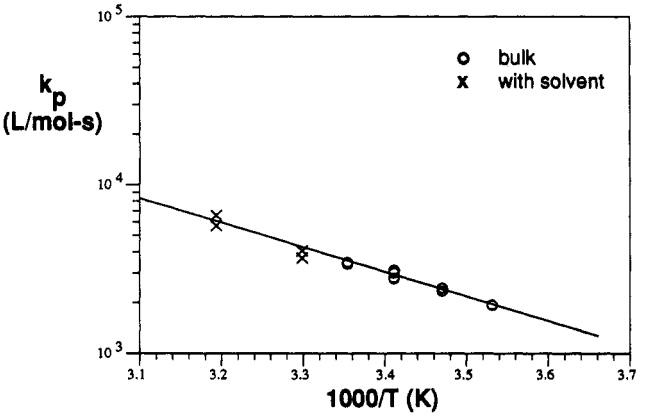

Figure 11. Arrhenius plot for the vinyl acetate propagation rate coefficient, as determined by PLP: (O, —) bulk VAc results and fit; (×) solution VAc results.

expected from eq 1, the inflection points increase with increasing VAc concentration. It can also be seen that the inflection points become harder to observe. However, by plotting M_o against the VAc fraction in the solution, it is possible to extrapolate to the pure VAc case, as illustrated by Figure 10 for 30 and 40 °C. The 30 and 40 °C k_p values calculated from these extrapolations are consistent with the Arrhenius relationship fit to the lower temperature data, given by eq 7 and plotted as Figure 11.

It is instructive to compare our PLP results with other reported values. Figure 12 plots the eq 7 Arrhenius relationship against a collection of data compiled in ref 16, as well as more recent results reported by Pernecker

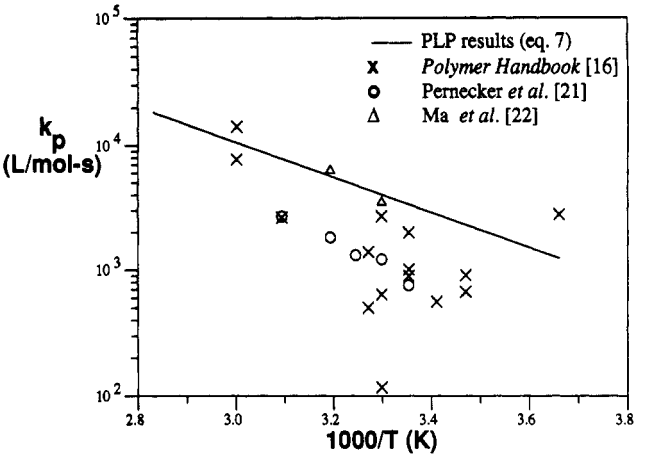

Figure 12. Comparison of PLP-determined vinyl acetate k_p values with other literature results.

et al.[21] and Ma *et al.*[22] The PLP determinations are toward the high end among the wide range of scatter. It is interesting to note that high k_p values in the literature are matched by high k_t estimates, while lower values are matched by corresponding lower k_t estimates. This correlation is not surprising, since most kinetic determinations measure a ratio of the two parameters, which are then resolved using another technique. The strength of the PLP/GPC method is that it gives a *direct* measurement of k_p, independent of k_t. Our results agree with the higher k_p estimates and thus support the conclusion that k_t must be large for VAc. The experimental sensitivity of the PVAc PLP-generated MWDs to initiator concentration also indicates the monomer has a very high rate of termination. MMA, on the other hand, has an estimated order of magnitude lower k_t value; the PMMA PLP-generated MWDs show much less sensitivity to [I] (compare Figure 4 with Figure 7).

Conclusions

The combination of high k_p and high k_t values makes VAc a difficult system to study with PLP. In order to obtain MWDs with an observable k_p peak, it is necessary to use very low concentrations of photoinitiator. Even under these conditions, however, inflection points are not always detectable, apparently due to the extreme sensitivity of the system to run-to-run variations in radical concentration.

Because of the less well-defined distributions (compared with MMA, for example), it proved impossible to estimate k_p from the number distribution, as described in our previous work.[3] Nonetheless, repetition of experiments and the consistency of k_p estimates at different photoinitiator and monomer concentrations establish the validity of the results.

This work extends the use of PLP with GPC analysis to high k_p systems. Through mathematical modeling, a better understanding of the relative importance of propagation, termination, and transfer events on the laser-generated MWDs has been developed. This insight led to a rational design of experiments and the direct measurement of k_p for VAc in the temperature range 10–40 °C. Simulations and experiments both suggest that VAc radicals not only propagate quickly but also have a faster rate of termination than methacrylate or styrene monomer systems. It is expected that the methodology developed in this work can easily be applied to examine other "difficult" systems, such as the acrylate family of monomers.

Acknowledgment. The authors would like to thank F. W. Bailey for running the PLP experiments, and R. Prybolsky and R. E. Fuller for prompt and reliable GPC analysis.

Appendix

This appendix details the equations used to represent the PLP system and the reduction of the model to interesting limiting cases. Chain balances are derived from the kinetic scheme presented in Figure 2. For initiator radicals

$$\frac{d[I^\bullet]}{dt} = [\Delta R^\bullet]\sum_{j=0}^{N}\delta(t - jt_o) - (k_i[M] + k_t\mu_0 + k_t[I^\bullet])[I^\bullet] \qquad [I^\bullet(0)] = [\Delta R^\bullet] \quad (8)$$

where $[\Delta R^\bullet]$ is the new radical concentration generated per laser pulse, $\delta(t)$ is the Dirac delta function defined such that $\int_{-\infty}^{\infty} f(t)\delta(t-a)\,dt = f(a)$, and k_t ($\equiv k_{t_d} + k_{t_c}$) is the total termination rate coefficient for disproportionation and coupling. The total growing polymer chain concentration is defined as $\mu_0 \equiv \sum_{n=1}^{\infty} P_n$.

For growing polymer of length 1

$$\frac{dP_1}{dt} = k_i[M][I^\bullet] - (k_p[M] + k_t\mu_0 + k_t[I^\bullet])P_1 + (k_{tr_m}[M] + k_{tr_s}[S])(\mu_0 - P_1), \qquad P_1(0) = 0 \quad (9)$$

For growing polymer of length n

$$\frac{dP_n}{dt} = k_p[M]P_{n-1} - (k_p[M] + k_{tr_m}[M] + k_{tr_s}[S] + k_t\mu_0 + k_t[I^\bullet])P_n, \qquad P_n(0) = 0, n \geq 2 \quad (10)$$

For dead polymer of length n

$$\frac{dD_n}{dt} = (k_{tr_m}[M] + k_{tr_s}[S] + k_{t_d}\mu_0 + k_t[I^\bullet])P_n + \frac{1}{2}k_{t_c}\sum_{m=1}^{n-1}P_mP_{n-m}, \qquad D_n(0) = 0, n \geq 2 \quad (11)$$

In the above equations, k_{tr_m} is the rate coefficient for transfer to the monomer [M] and k_{tr_s} is the rate coefficient for transfer to the solvent [S].

The chain balances (eqs 9–11) are not sufficient to describe the system since an arbitrary stopping chain length (e.g., 7500) must be chosen. In order to complete the description and to calculate chain fractions for MWDs, it is necessary to follow *total* polymer concentrations. The method of moments[18] is used:

$$\mu_0 \equiv \sum_{n=1}^{\infty} P_n$$

$$\frac{d\mu_0}{dt} = k_i[M][I^\bullet] - k_t\mu_0(\mu_0 + [I^\bullet]), \qquad \mu_0(0) = 0 \quad (12)$$

$$\lambda_0 \equiv \sum_{n=1}^{\infty}(D_n + P_n)$$

$$\frac{d\lambda_0}{dt} = k_i[M][I^\bullet] + k_{tr_m}[M]\mu_0 + k_{tr_s}[S]\mu_0 - \frac{1}{2}k_{t_c}\mu_0^2, \qquad \lambda_0(0) = 0 \quad (13)$$

$$\lambda_1 \equiv \sum_{n=1}^{\infty} n(D_n + P_n)$$

$$\frac{d\lambda_1}{dt} = -\frac{d[M]}{dt} = k_i[M][I^\bullet] + k_{tr_m}[M]\mu_0 + k_{tr_s}[S]\mu_0 + k_p[M]\mu_0, \qquad \lambda_1(0) = 0 \quad (14)$$

During PLP experiments, where conversion is only carried out to about 1%, the decrease in monomer concentration is negligible ($[M] = [M]_0 - \lambda_1$). The bulk moments λ_0 and λ_1 are used in the calculation of number ($f(n)$) and weight ($w(n)$) chain fractions:

$$f(n) = D_n/\lambda_0 \quad (15)$$

$$w(n) = nD_n/\lambda_1 \quad (16)$$

The transformation to log distribution is done as before:[3]

$$w(\log n) = \ln 10\, nw(n) \quad (17)$$

Pseudo-Steady-State Limiting Case. Summing eqs 8 and 12 yields an expression for the total radical concentration ($[R^\bullet] \equiv [I^\bullet] + \mu_0$):

$$\frac{d[R^\bullet]}{dt} = \Delta[R^\bullet]\sum_{j=0}^{N}\delta(t - jt_o) - k_t[R^\bullet]^2, \qquad [R^\bullet(0)] = [\Delta R^\bullet] \quad (18)$$

Integrating this equation using the properties of the delta function from $(j-1)t_o$ to jt_o (between two consecutive pulses) yields the fraction of radicals which has escaped termination:[1]

$$\beta \equiv \frac{[R^\bullet(jt_o)]}{[R^\bullet]_{max}} = \frac{1}{1 + k_t[R^\bullet]_{max}t_o} \quad (19)$$

where $[R^\bullet(jt_o)]$ represents the radical fraction at the instant before the jth pulse and $[R^\bullet]_{max}$ is the radical concentration immediately following the $(j-1)$th laser pulse. When a pseudostationary radical profile has been obtained,[1] $[R^\bullet]_{max}$ is related to $[\Delta R^\bullet]$ by

$$[R^\bullet]_{max} = [\Delta R^\bullet]\left(\frac{1}{2} + \sqrt{\left(\frac{1}{4} + \frac{1}{k_t t_o[\Delta R^\bullet]}\right)}\right) \quad (20)$$

with $[R^\bullet]_{max} - [R^\bullet(jt_o)] = [\Delta R^\bullet]$.

Poisson MWD Limiting Case. Consider the case with $k_t = k_{tr_m} = k_{tr_s} = 0$ and $k_i \to \infty$. Equations 9 and 10 reduce to a "living" system following a single pulse of radical generation:

$$\frac{dP_1}{dt} = -k_p[M]P_1, \qquad P_1(0) = [\Delta R^\bullet] \quad (21)$$

$$\frac{dP_n}{dt} = k_p[M](P_{n-1} - P_n), \qquad P_n(0) = 0, n \geq 2 \quad (22)$$

This case has the immediate solution[18]

$$P_n = [\Delta R^\bullet]e^{-k_p[M]t}\frac{(k_p[M]t)^{n-1}}{(n-1)}, \qquad n \geq 1 \quad (23)$$

with $(k_p[M]t)$ the mean chain length at any time. This

limiting Poisson case has been used to validate the numerical solution of the model.

References and Notes

(1) Olaj, O. F.; Bitai, I.; Hinkelmann, F. *Makromol. Chem.* **1987**, *188*, 1689.
(2) Olaj, O. F.; Schnöll-Bitai, I. *Eur. Polym. J.* **1989**, *25*, 635.
(3) Hutchinson, R. A.; Aronson, M. T.; Richards, J. R. *Macromolecules* **1993**, *26*, 6410.
(4) Davis, T. P.; O'Driscoll, K. F.; Piton, M. C.; Winnik, M. A. *Macromolecules* **1990**, *23*, 2113.
(5) Pascal, P.; Winnik, M. A.; Napper, D. H.; Gilbert, R. G. *Makromol. Chem., Rapid Commun.* **1993**, *14*, 213.
(6) Beuermann, S.; Russell, G. T.; Buback, M. *Makromol. Chem., Rapid Commun.* **1994**, *15*, 351.
(7) Manders, B. G.; van Herk, A. M.; German, A. L.; Sarnecki, J.; Schomäcker, R.; Schweer, J. *Makromol. Chem., Rapid Commun.* **1993**, *14*, 693.
(8) Deady, M.; Mau, A. W. H.; Moad, G.; Spurling, T. H. *Makromol. Chem.* **1993**, *194*, 1691.
(9) Davis, T. P.; O'Driscoll, K. F.; Piton, M. C.; Winnik, M. A. *Macromolecules* **1989**, *22*, 2785.
(10) Morrison, B. R.; Piton, M. C.; Winnik, M. A.; Gilbert, R. G.; Napper, D. H. *Macromolecules* **1993**, *26*, 4368.
(11) Davis, T. P.; O'Driscoll, K. F.; Piton, M. C.; Winnik, M. A. *Polym. Int.* **1991**, *24*, 65.
(12) Lu, J.; Zhang, H.; Yang, Y. *Makromol. Chem., Theory Simul.* **1993**, *2*, 747.
(13) O'Driscoll, K. F.; Kuindersma, M. E. *Makromol. Chem., Theory Simul.* **1994**, *3*, 469.
(14) Atkinson, C. M. L.; Dietz, R. *Eur. Polym. J.* **1979**, *15*, 21.
(15) *IMSL Problem-Solving Software Systems Math/Library User's Manual*, Version 1.0; IMSL, Inc.: Houston, TX, 1987.
(16) *Polymer Handbook*, 3rd ed.; Brandrup, J., Immergut, E. H., Eds.; Wiley-Interscience: New York, 1989.
(17) Matheson, M. S.; Auer, E. E.; Bevilacqua, E. B.; Hart, E. J. *J. Am. Chem. Soc.* **1949**, *71*, 2610.
(18) Ray, W. H. *J. Macromol. Sci.—Rev. Macromol. Chem.* **1972**, *C8*, 1.
(19) Hutchinson, R. A. *Polym. React. Eng.* **1993**, *1*, 521.
(20) Tung, L. H. *J. Appl. Polym. Sci.* **1966**, *10*, 375.
(21) Pernecker, T.; Foldes-Berezsnich, T.; Tudos, F. *J. Macromol. Sci., Chem.* **1990**, *A27*, 1029.
(22) Ma, Y.-D.; Won, Y.-C.; Kubo, K.; Fukuda, T. *Macromolecules* **1993**, *26*, 6766.
(23) Zifferer, G.; Olaj, O. F. *Makromol. Chem.* **1990**, *191*, 1699.